# Commensurate and incommensurate magnetic order in $Fe_{1+y}Te$

Gang Chen
in collaboration with Leo Radzihovsky

# Outline

- Motivation
- Our theoretical model and prediction
- Our interpretation of the experiments
- Conclusion

# Tunable ($\delta\pi$, $\delta\pi$)-Type Antiferromagnetic Order in $\alpha$-Fe(Te,Se) Superconductors

Wei Bao,[1,2,*] Y. Qiu,[3,4] Q. Huang,[3] M. A. Green,[3,4] P. Zajdel,[3,5] M. R. Fitzsimmons,[2] M. Zhernenkov,[2] S. Chang,[3] Minghu Fang,[6,7] B. Qian,[6] E. K. Vehstedt,[6] Jinhu Yang,[7] H. M. Pham,[8] L. Spinu,[8] and Z. Q. Mao[6]

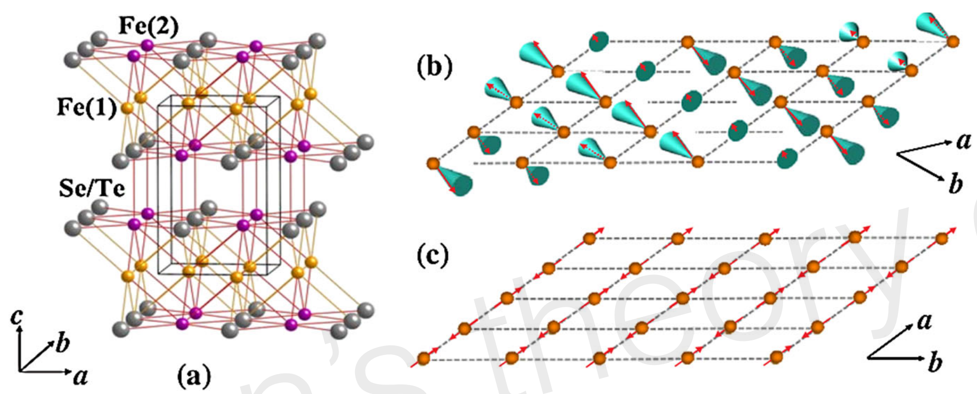


FIG. 1 (color online). (a) Crystal structure of $\alpha$-Fe(Te,Se). Magnetic structures of (b) $\alpha$-FeTe and (c) $BaFe_2As_2$ are shown in the *primitive* Fe square lattice for comparison. Note that the basal square lattice of the PbO unit cell in (a) is a $\sqrt{2} \times \sqrt{2}$ superlattice of that in (b).

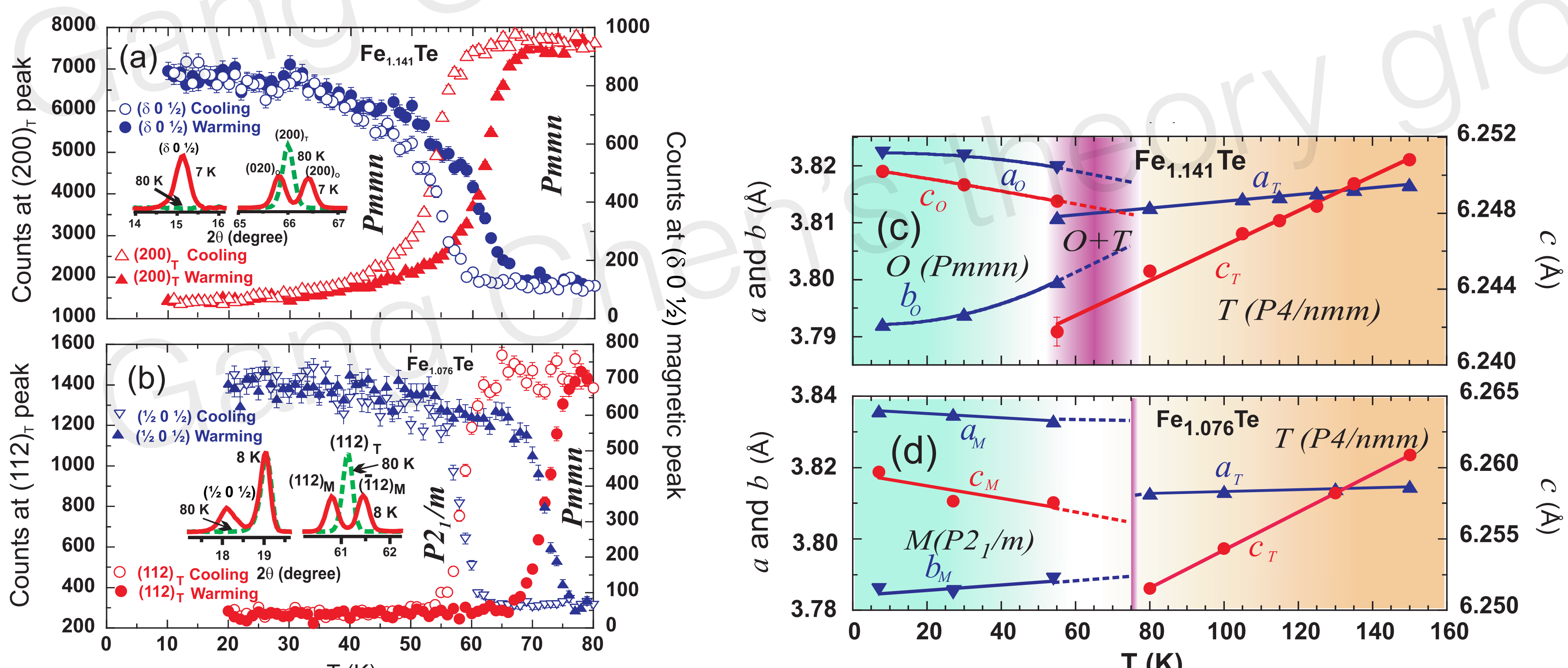


FIG. 3 (color online). (a),(b) The magnetic Bragg peak ($\delta$, 0, 1/2) (blue symbols) and the splitting of the structural peak (200) or (112) of the tetragonal phase (red symbols) show the thermal hysteresis in the first-order transition. (c),(d) The lattice parameters through the transition.

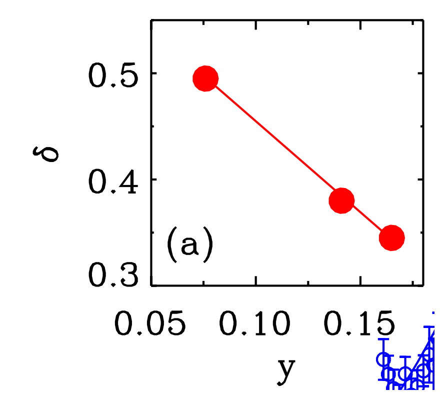

# Dimtry’s neutron experiments

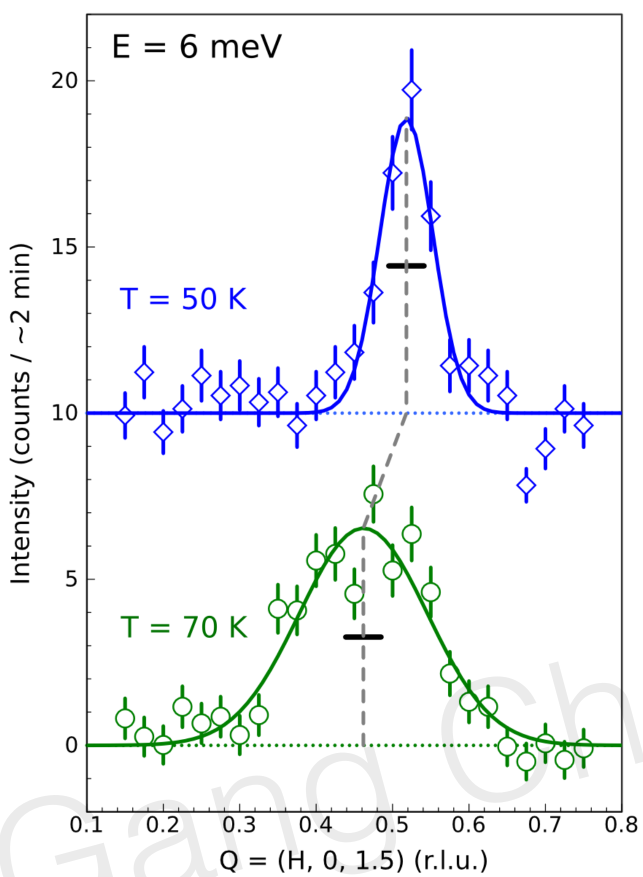


FIG. 1. Scans through (H, 0, 0.5) with E = 6 meV, taken above and below $T_N = 67.5$ K. The black horizontal bar shows the estimated resolution width.

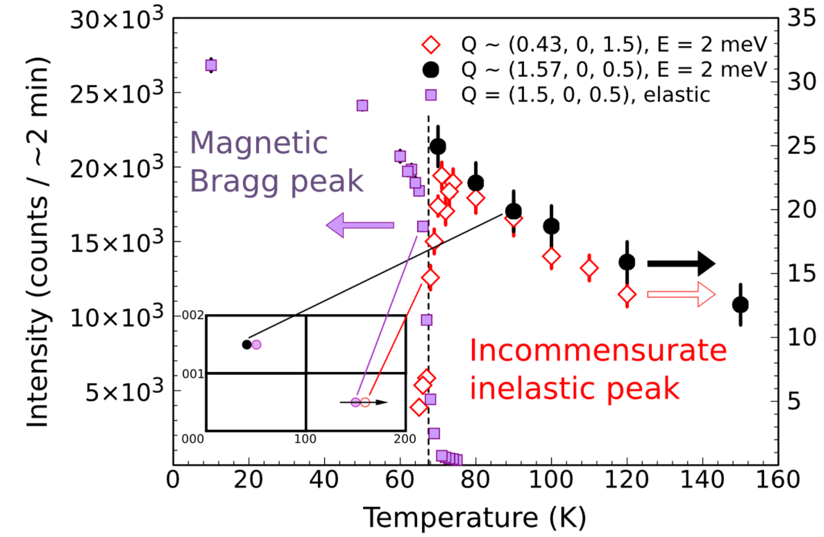


FIG. 2. a) Peak intensities of the incommensurate magnetic excitation and the magnetic Bragg peak as a function of temperature. Inset: width of (004) Bragg peak as a function of temperature, showing the structural transition at 67.5 K. b) some more scans

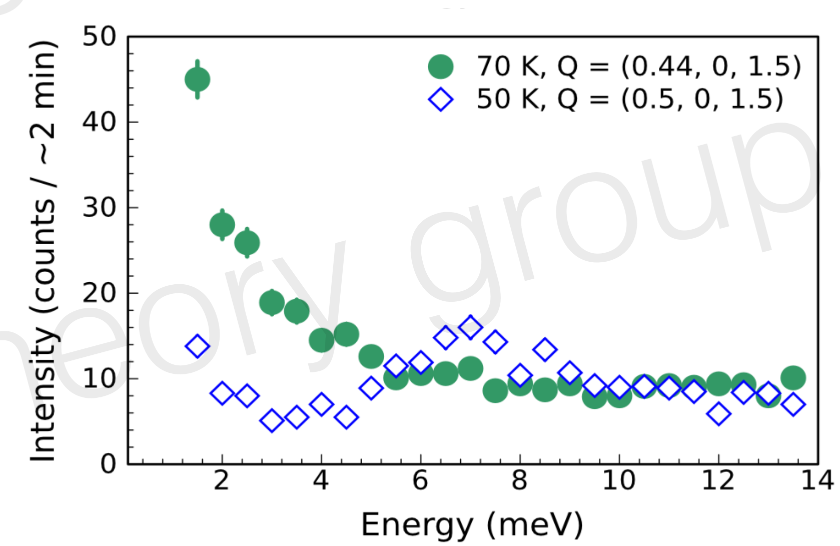

# Interstitial iron tuning of the spin fluctuations in $Fe_{1+x}Te$

Chris Stock,[1,2] Efrain E. Rodriguez,[1] Mark A. Green,[1,3] Peter Zavalij,[4] and Jose A. Rodriguez-Rivera[1,3]

[1] *NIST Center for Neutron Research, National Institute of Standards and Technology, 100 Bureau Dr., Gaithersburg, MD 20889*
[2] *Indiana University Cyclotron Facility, 2401 Milo B. Sampson Lane, Bloomington, IN 47404*
[3] *Department of Materials Science and Engineering, University of Maryland, College Park, MD 20742*
[4] *Department of Chemistry, University of Maryland, College Park, MD 20742*

(Dated: April 1, 2011)

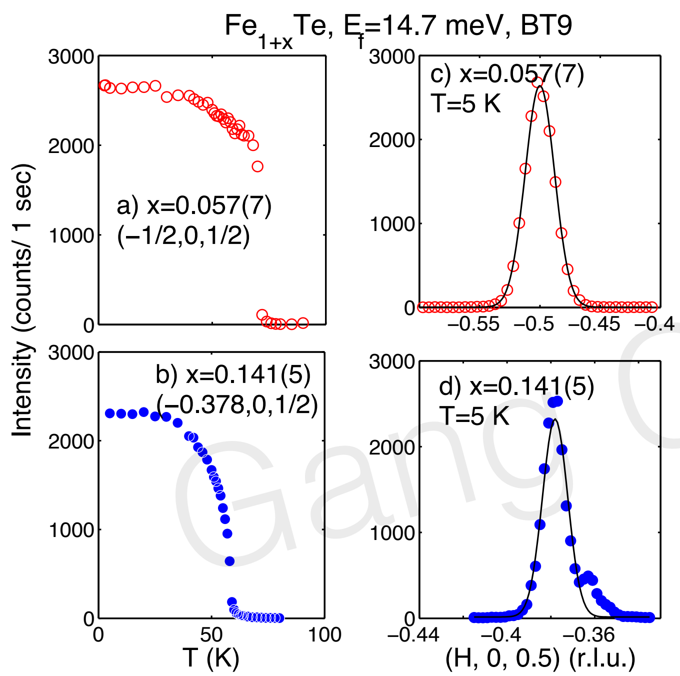


FIG. 1. The temperature and momentum dependence of the elastic magnetic scattering measured in $Fe_{1.057(7)}Te$ (*a* and *c*) and $Fe_{1.141(5)}Te$(*b* and *d*)) taken on warming. The data were taken with graphite filters and 80' collimators placed before and after the sample using BT9. The solid lines represent fits to resolution limited gaussian line shapes.

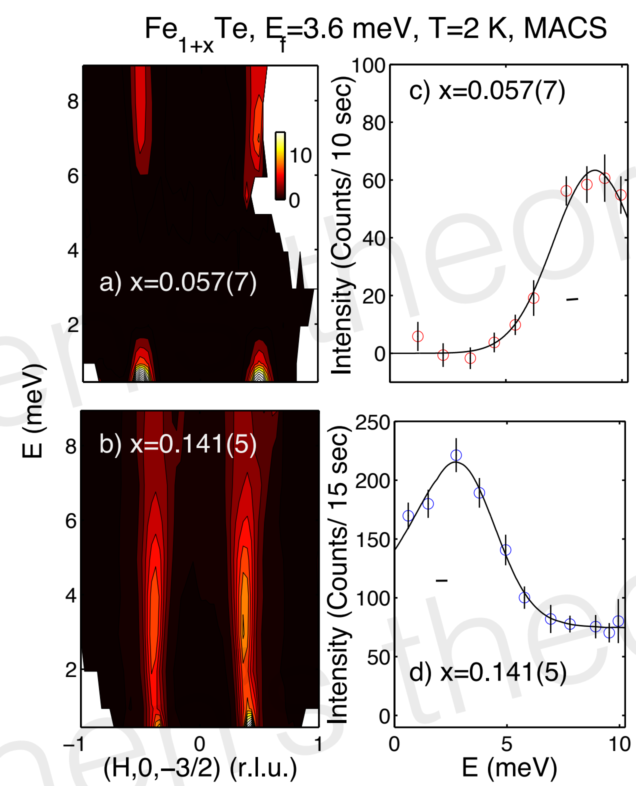


FIG. 2. Constant-Q slices (*a* and *b*) and constant-Q scans obtained using the MACS cold triple-axis spectrometer. *a* and *b* are integrated over L=[-1.525,-1.475]. Constant-Q cuts are displayed in panels *c* and *d*. Panel *c* integrates over H=[-0.55,-0.45] and L=[-1.55,-1.45]. Panel *d* integrates over H=[-0.4,-0.36] and L=[-1.55,-1.45]. The solid curves are guides to the eye.

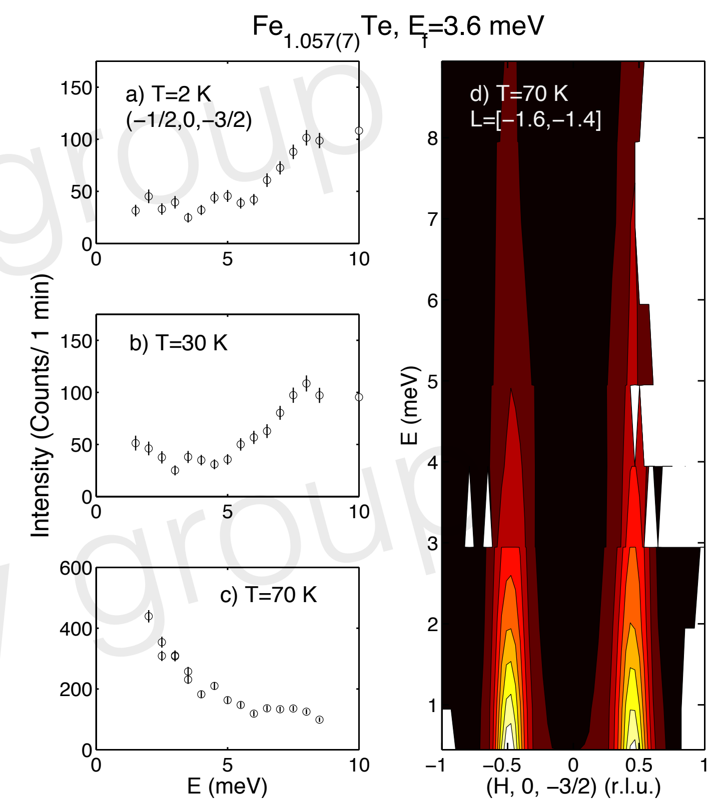


FIG. 5. The temperature dependence of the magnetic excitations in $Fe_{1.057(7)}Te$. The constant-Q scans in $a - c$ where taken with a single detector channel on MACS at T=2, 30, and 70 K. *d* illustrates a constant-Q slice taken at 70 K illustrating the gapless excitations.

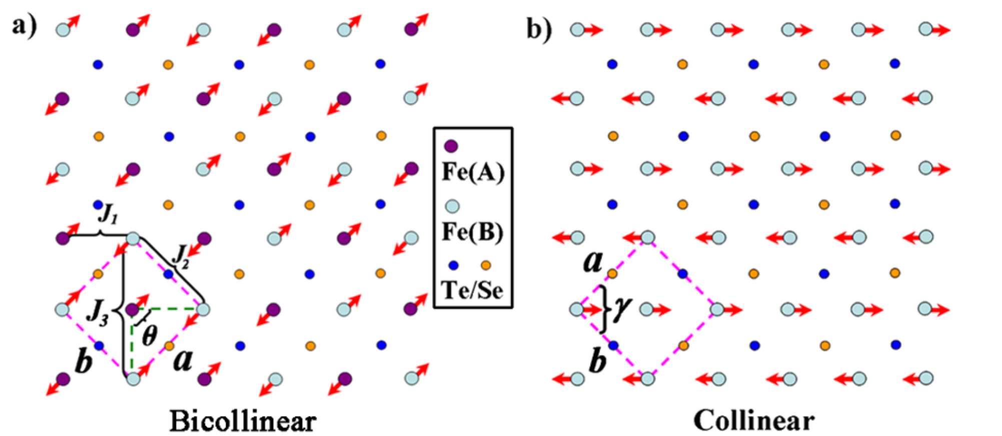


FIG. 1 (color online). Schematic representations of magnetic orders in the ground states of (a) $\alpha$-FeTe and (b) $\alpha$-FeSe. The Fe spins are shown by red arrows. The bicollinear antiferromagnetic (AFM) order means that the Fe moments align ferromagnetically along a diagonal direction and antiferromagnetically along the other diagonal direction on the Fe-Fe square lattice. In other words, if the Fe-Fe square lattice is divided into two square sublattices $A$ and $B$, the Fe moments on each sublattice take their own collinear AFM order.



Info from experiments:

1. Unusual bi-collinear spin order along b axis for low Fe doping
2. Large spin-wave gap for the bi-collinear state
3. Incommensurate spin spiral state for high Fe doping
4. Gapless spin wave excitation for the incommensurate phase
5. Incommensurate spin fluctuation above the Tc
6. Strong correlation between spin, orbital and crystal structure

Gang Chen's theory group

# Others' theory

C. Fang, B. A. Bernevig and Jiangping Hu, **EPL 2009**

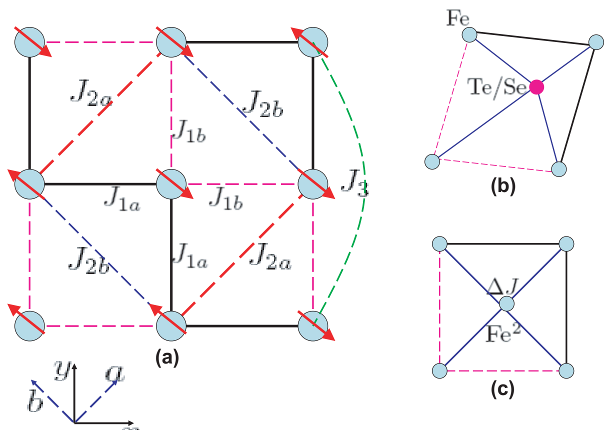


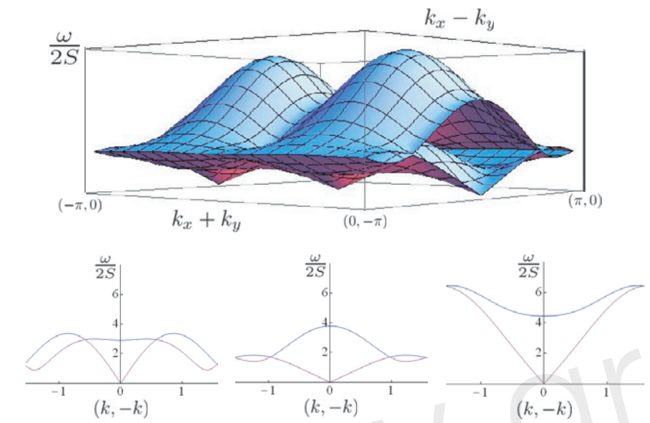


A.M. Turner, F. Wang and Ashvin Vishwanath **PRB 2009**

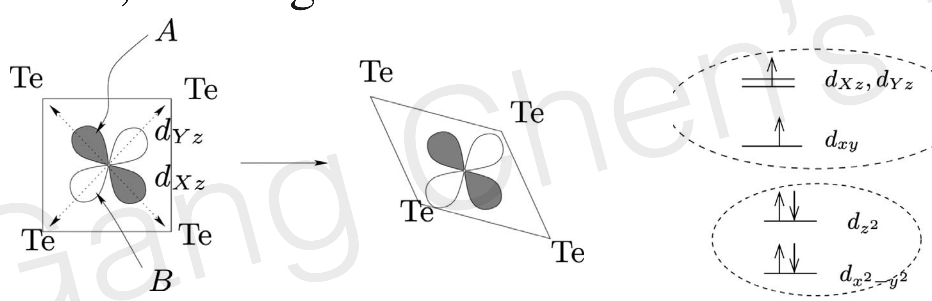


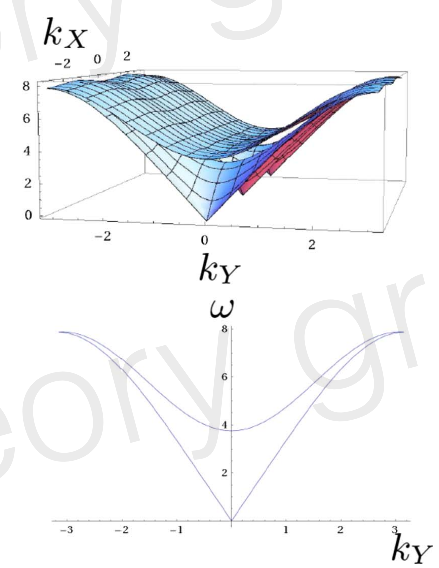


$$H = \sum_{ij} J_{ij} \mathbf{S}_i \cdot \mathbf{S}_j - K \sum_{\langle ij \rangle} (\mathbf{S}_i \cdot \mathbf{S}_j)^2.$$

Wei-Guo Yin,* Chi-Cheng Lee, and Wei Ku PRL 2010

The minimum model considered is an effective orbital-degenerate double-exchange model [23]:

$$H = -\sum_{ij\gamma\gamma'\mu} (t_{ij}^{\gamma\gamma'} C_{i\gamma\mu}^{\dagger} C_{j\gamma'\mu} + \text{H.c.}) - \frac{K}{2} \sum_{i\gamma\mu\mu'} C_{i\gamma\mu}^{\dagger} \vec{\sigma}_{\mu\mu'} C_{i\gamma\mu'} \cdot \vec{S}_i + \sum_{ij} J_{ij} \vec{S}_i \cdot \vec{S}_j, \quad (1)$$

# Our theoretical model

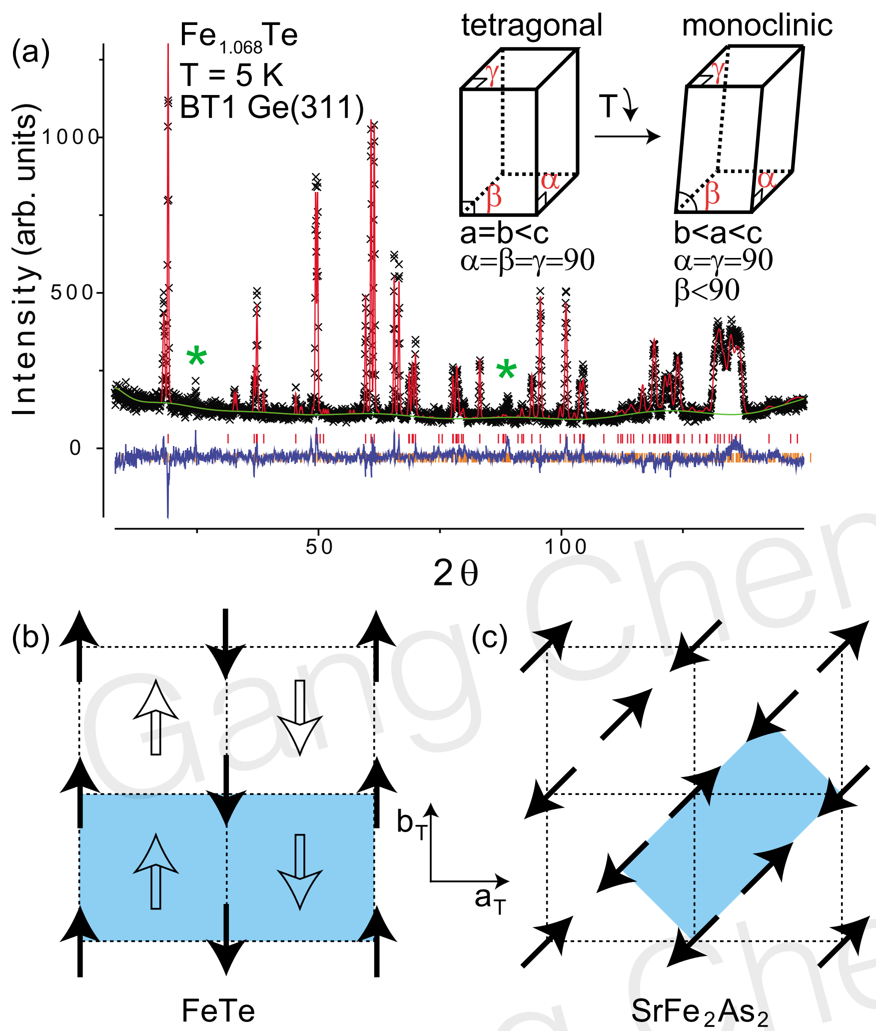


$$\mathcal{H}_{\rm ex} = J_1 \sum_{\langle ij \rangle} \mathbf{S}_i \cdot \mathbf{S}_j + J_{2a} \sum_{\langle\langle ij \rangle\rangle_a} \mathbf{S}_i \cdot \mathbf{S}_j - J_{2b} \sum_{\langle\langle ij \rangle\rangle_b} \mathbf{S}_i \cdot \mathbf{S}_j.$$

$$\mathcal{H}_{\rm ani} = -\sum_i [A_a (S_i^a)^2 + A_b (S_i^b)^2]$$

Three candidate ground states:

1. (Pi,Pi) Neel
2. (Pi/2, -Pi/2) bi-collinear
3. (k,-k) incommensurate spin spiral

$$E(k,-k)|_{\cos k = -J_1/(2J_{2a})} = -(J_{2a}+J_{2b}+\frac{J_1^2}{2J_{2a}}) - \frac{A_a + A_b}{2}$$

$$E(\pi/2, -\pi/2) = -(J_{2a} + J_{2b}) - A_b$$

$$E(k,-k)|_{\cos k = -J_1/(2J_{2a})} = -(J_{2a}+J_{2b}+\frac{J_1^2}{2J_{2a}}) - \frac{A_a + A_b}{2}.$$


Gang Chen's theory group

spin wave dispersion (see mathematica)

# Commensurate-incommensurate transition

Hubbard-Stratonovich xform

$$\mathcal{Z} = \int \mathcal{D}\phi \, e^{\beta J_{ij}^{-1} \boldsymbol{\phi}_i \cdot \boldsymbol{\phi}_j /2} \mathrm{Tr}\, e^{-\beta \mathcal{H}_{\text{ani}} - \beta \sum_i \mathbf{S}_i \cdot \boldsymbol{\phi}_i}$$

$$\boldsymbol{\phi}_\mu(\mathbf{r}_i) = e^{i\frac{\pi}{2}(x_i - y_i)} \boldsymbol{\psi}_\mu(\mathbf{r}_i)$$

$$\begin{aligned} f^{(2)}[(\psi)] = &- \sum_{\mu=0,1} (-)^\mu \Big(\frac{(\psi_\mu^a)^2}{A_b} + \frac{(\psi_\mu^b)^2}{A_a}\Big) \\ &+ \sum_{\mu=0,1} \frac{(-)^\mu}{2} \psi_\mu^\alpha (-c_0 + c_X \partial_X^2 + c_Y \partial_Y^2) \psi_\mu^\alpha \\ &+ \gamma \psi_A^\alpha (i\partial_Y) \psi_B^\alpha, \end{aligned} \tag{24}$$

$$\begin{aligned} f^{(4)}[(\psi)] = &\sum_\mu \frac{(\psi_\mu^a)^4}{A_b^3} + \frac{(\psi_\mu^b)^4}{A_a^3} + \frac{(\psi_\mu^a)^2 (\psi_\mu^b)^2}{A_a A_b} \Big(\frac{1}{A_a} + \frac{1}{A_b}\Big) \\ &- \frac{(\psi_\mu^z)^2}{A_a A_b} \Big(\frac{(\psi_\mu^a)^2}{A_b} + \frac{(\psi_\mu^b)^2}{A_a}\Big) \end{aligned} \tag{29}$$

$$\begin{aligned} \psi_A^b &= \psi^b \cos(\delta Y + \theta_b) \\ \psi_B^b &= (-i) \psi^b \sin(\delta Y + \theta_b), \end{aligned}$$

$$\begin{aligned} \boldsymbol{\psi}_A &= \psi_0 \mathrm{Re}[(\hat{a} + i\hat{b}) e^{i(\delta Y + \theta)}] \\ \boldsymbol{\psi}_B &= (-i) \psi_0 \mathrm{Re}[(-\hat{b} + i\hat{a}) e^{i(\delta Y + \theta)}] \end{aligned}$$

$$f = \frac{\kappa}{2} (\partial_Y \theta)^2 + \sigma \cos 4(\theta + \delta Y)$$

$$\delta_c = \frac{2}{\pi} \sqrt{\frac{\sigma}{\kappa}}.$$

# In external magnetic field

$$\mathcal{H} = \mathcal{H}_{\text{ex}} + \mathcal{H}_{\text{ani}} - \sum_i \mathbf{B} \cdot \mathbf{S}_i$$

## 1. bi-collinear state

### A. Field along c/z direction

$$\mathbf{S}_{A,i} = (-)^{(x-y)/2} m_s \hat{b} + m\hat{z}$$
$$\mathbf{S}_{B,i} = (-)^{(x-y-1)/2} m_s \hat{b} + m\hat{z},$$
$$m = \frac{B}{2(2J_1 + 2J_{2a} + A_b)} \tag{42}$$
$$E_c^z(B) = -(J_{2a} + J_{2b} + A_b) - \frac{B^2}{4(2J_1 + 2J_{2a} + A_b)} \tag{43}$$

### B. Field along b direction: spin-flop transition

$$\mathbf{S}_{A,i} = (-)^{(x-y)/2} m_s \hat{a} + m\hat{b}$$
$$\mathbf{S}_{B,i} = (-)^{(x-y-1)/2} m_s \hat{a} + m\hat{b}.$$

$$B_c = 2\sqrt{(A_b - A_a)(2J_1 + 2J_{2a} + A_a - A_b)}.$$

$$m = \frac{B}{2(2J_1 + 2J_{2a} + A_a - A_b)} \tag{46}$$
$$E_c^b = -(J_{2a} + J_{2b} + A_a) - \frac{B^2}{4(2J_1 + 2J_{2a} + A_a - A_b)} \tag{47}$$

### C. Field along a direction

$$\mathbf{S}_{A,i} = (-)^{(x-y)/2} m_s \hat{b} + m\hat{a}$$
$$\mathbf{S}_{B,i} = (-)^{(x-y-1)/2} m_s \hat{b} + m\hat{a}.$$

$$m = \frac{B}{2(2J_1 + 2J_{2a} + A_b - A_a)} \tag{51}$$
$$E_c^a = -(J_{2a} + J_{2b} + A_b) - \frac{B^2}{4(2J_1 + 2J_{2a} + A_b - A_a)} \tag{52}$$

## 2. Incommensurae spin spirals

Interpretation of experiments

1. Unusual bi-collinear spin order along b axis for low Fe doping
2. Large spin-wave gap for the bi-collinear state
3. Incommensurate spin spiral state for high Fe doping
4. Gapless spin wave excitation for the incommensurate phase
5. Incommensurate spin fluctuation above the Tc
6. Strong correlation between spin, orbital and crystal structure

# Conclusion

1. Our model explain many experimental observation: different spin orders, spin wave excitation, etc.

2. Our model gives prediction for further experimental direction.